Bioactivity and Antibacterial Effects of Ag-Ca-P Doped PEO Titania Coatings

Luciane S. Santos[1], Dhanna Francisco[1], Evelyn Leite[2], Sheron Cogo[3,4], Marcela Dias-Netipanyj[3,4], Shelon Pinto[2], Selene Espósito[3], Ketul Popat[4] and Paulo Soares[1,*]

[1]*Department of Mechanical Engineering, Polytechnic School, Pontifícia Universidade Católica do Paraná, Curitiba – PR 80215-901 Brazil*

[2]*Dentistry Department, Universidade Estadual de Ponta Grossa, Ponta Grossa - PR, 84010-290 Brazil*

[3]*Health Science Department, Pontifícia Universidade Católica do Paraná, Curitiba – PR 80215-901 Brazil*

[4]*Department of Mechanical Engineering, School of Biomedical Engineering, Colorado State University, Fort Collins, CO 80523 USA*

Abstract: Implant centered infections remain as one of the main complications associated with the use of biomedical implants. These infections can be avoided with the development of bactericidal coatings that prevent bacterial contamination since the very early stage of implantation. However, a multifunctional coating should inhibit bacterial contamination without generating cytotoxic responses. To achieve this purpose, this work presents a comparative evaluation of coatings with different concentrations of Ag. Coatings containing silver, calcium and phosphorous were obtained by plasma electrolytic oxidation (PEO) and its bactericidal activity and cytotoxicity were evaluated against Staphylococcus aureus and adipose derived stem cells (ADSC), respectively. Silver, calcium and phosphorous were successfully incorporated in the coatings and silver has not affected the coating morphology nor the crystalline structure. ADSC viability was unaltered by cell growth over the surfaces, despite the observation of thinner cells on coatings with higher silver content. After 24 h of incubation, bactericidal activity was observed in coatings with more than 0.6 % at. Ag incorporated, while coatings with 0.2 % at. Ag presented an increased bacterial proliferation indicating a hormetic response. Thus, Ag-CaP-TiO2 coating could be a potential solution for the prevention of implant infections.

Keywords: Plasma electrolytic oxidation, titanium, bactericidal coating, silver.

1. INTRODUCTION

Metallic implants are prone to bacterial contamination during and after surgery, leading to implant centered infections (ICI) [1-3]. The current ICI treatment of ICI consists of long antibiotic therapies and revision surgeries, representing a clinical challenge and an economic burden for health care systems [4-6]. Despite the efforts to avoid the bacterial contamination, the ICI still has high rates of occurrence and mortality [7–9].

The use of bactericidal coatings on metallic implants represent a long term alternative to avoid bacterial contamination [10]. Many researchers have suggested the use of silver based coatings, as this element presents a broad spectrum bactericidal activity [11-14]. The bactericidal mechanism of silver is not fully understood yet, but it is well known that silver ions can interact with thiol groups (S-H) forming Ag-S bonds. Thiol groups are present in many proteins and its disruptions lead to loss of proteins shape and functionality [15,16]. Silver also kills bacteria by generating reactive oxygen species (ROS) which impairs enzymes from the respiratory chain and prevents DNA replication [17]. Silver is used as a bactericidal agent in air disinfection systems, water filters and food package, but the use of silver in indwelling devices remain controversial as some cytotoxic reactions can be originated [18-23]. Studies *in vitro* showed that silver nanoparticles decrease liver cells viability by ROS generation, inducing cells to apoptosis [24,25]. A case study conducted by Trop *et al*. [26], had also showed the increase of silver levels in blood and a higher production of liver enzymes when silver based wound dressings were used for burn healing. Furthermore, the indiscriminate use of silver can induce argyria, a cutaneous manifestation where silver precipitates are deposited on the skin, giving it a brownish-grey appearance [27-29]. As the use of bactericidal coatings in endosseous implants must not damage eukaryotic cells around the implant, and silver has a dose-dependent cytotoxicity, a systematic investigation of the proper amount of silver in implants is needed in order not to impair osseointegration [30,31].

An effective technique to incorporate elements on the surface of titanium implants is the plasma

*Address correspondence to this author at the Pontifícia Universidade Católica do Paraná, Department of Mechanical Engineering, Rua Imaculada Conceição, 1155 – Prado Velho, Curitiba, PR – 80710-230, Brazil; Tel: +55 (41) 3271-1338; E-mail: pa.soares@pucpr.br

E-ISSN: 2311-1755/18

electrolytic oxidation (PEO) [32-34]. This technique produces a well adhered rough coating on the implant surface and it is possible to change the coating properties by selecting the appropriate oxidation parameters [35, 36]. PEO is widely used to obtain calcium and phosphorous doped coatings, as these elements improve the bone apposition after the implantation [37-39]. By adding bactericidal elements along with calcium and phosphorous sources in the electrolyte it is possible to adjust oxidation parameters to obtain a bactericidal and biocompatible coating.

The aim of this work is to obtain Ag-Ca-P doped coatings by PEO and evaluate the influence of silver concentration on bactericidal activity and biocompatibility *in vitro*, as well as to determine the minimum silver concentration needed to assure bactericidal activity without compromising the biocompatibility.

2. MATERIALS AND METHODS

2.1. Sample Preparation

Commercially pure Ti disks (ø 12 mm) were grinded with #600 SiC abrasive paper and ultrasonically cleaned in acetone, ethanol and deionized water. Coatings were obtained by PEO using a DC power supply (Model 62012P-600-8, Chroma). Oxidation was carried out in potentiostatic mode at 350 V for 60 s in room temperature, using a Ti plate as counter electrode. Table **1** lists the different electrolyte compositions, where CaP denotes the coating obtained without Ag in the electrolyte and 2Ag-CaP, 4Ag-CaP, 16Ag-CaP and 64Ag-CaP stands for coatings obtained with different Ag concentrations in the electrolyte. A CaP sample was used as a standard control sample for all the assays. After the PEO treatment, samples were washed with deionized water and air dried.

2.2. Coating Characterization

The coating morphology and chemical composition were evaluated by scanning electron microscopy (SEM, Vega3, Tescan) and X-ray photoelectron spectroscopy (XPS, Physical Electronics PHI-5800 spectrometer). For XPS, all spectra were referenced by setting the C 1s peak to 284.6 eV to compensate for residual charging effects. Survey spectra were collected from 0 to 1100 eV with a pass energy of 187.85 eV. Data for percent elemental composition, elemental ratios and peak fit analysis were calculated using Multipack and XPS Peak 4.1 (Freeware) software. X-ray diffraction (XRD, XRD-7000 Shimadzu) using a CuKα radiation at 40 kV and 30 mA with a fixed incidence angle of 5°, was used in thin film (TF-XRD) mode to determine coatings crystalline phases.

2.3. Cell Culture

Before biological assays, the samples were cleaned and sterilized in a sequence of acetone, alcohol and phosphate buffered saline (PBS), followed by 30 min UV radiation exposure.

Adipose derived stem cells (ADSCs) were cultured in α-MEM medium, supplemented with 10% Fetal Bovine Serum (FBS) and 1% penicillin-streptomycin in a humidified incubator at 5% CO2 and 37 °C. Samples were independently allocated in the wells of a 48-well plate and ADSCs were seeded into the coatings at a density of 10^4 cells per well.

2.4. Cell Viability Assay

To determine the effect of silver content present in the coatings on ADSCs viability, AlamarBlue (Promega) assay was performed after 1 and 7 days. Samples with adhered cells were incubated at 37 °C for 4 h in culture media and 10% of Alamar Blue Reagent. After 4 h, the solution optical density (OD) was measured at 570 nm and 600 nm using a spectrophotometer (FLUO-star Omega; BMG Labtech). The percentage reduction of Alamar Blue was calculated following the manufacturer instructions. The data was statistically analyzed by one-way ANOVA with Tukey's test.

Table 1: Electrolyte Composition Used in the PEO Process

Sample name	Electrolyte composition (L^{-1})		
	Silver nitrate	Calcium acetate	Calcium Glycerophosphate
CaP	-	0.15 M	0.02 M
2Ag-CaP	0.02 mM	0.15 M	0.02 M
4Ag-CaP	0.04 mM	0.15 M	0.02 M
16Ag-CaP	0.16 mM	0.15 M	0.02 M
64Ag-CaP	0.64 mM	0.15 M	0.02 M

2.5. Cell Adhesion and Proliferation

After 1 and 7 days of initial culture, the cell adhesion and proliferation were investigated by fluorescence staining with Rhodamine Phalloidin and 4' 6-diamidino-2-phenylindole DAPI. Rhodamine dyes the cell cytoskeleton red, by having a high affinity F-actin probe coupled with a red fluorescent dye, whereas DAPI reveals cells nuclei by staining its DNA with blue.

The coatings were removed from the culture media, washed with PBS and fixed with 3.7% of formaldehyde for 15 min at room temperature. To permeabilize cells, the coatings were incubated with 1% of Triton-X100 for 3 min, and then washed with PBS. The surfaces were incubated in 70 nM rhodamine-phalloidin for 30 min at room temperature. After 25 min of rhodamine-phalloidin staining, 300 nM DAPI was added for 5 min. All the solution was aspirated, and the surfaces were washed with PBS, and imaged using a Zeiss Imager-A2 fluorescence microscope.

2.6. Cell Morphology

After 1 and 7 days of culture, cells were fixed in a solution of 3% glutaraldehyde (Ted Pella), 0.1 M sodium cacodylate (Alfa Aesar), and 0.1 M sucrose (Fisher Scientific) for 45 min. The samples were incubated in buffer solution of 0.1 M sodium cacodylate (Alfa Aesar) and 0.1 M sucrose (Fisher Scientific) for 10 min. After fixation, the cells were dehydrated in series of ethanol solutions for 10 min each and incubated in dexamethyldisilazane (HMDS, Sigma) for 10 min. Prior to observation in the SEM, the samples were coated with 20 nm of gold. Cells SEM images were recorded with a 45° tilt.

2.7. Bacteria Culture

Staphylococcus aureus (ATCC 25923) was cultivated in brain heart infusion (BHI) agar medium (Acumedia®, 107340A) for 24 h at 37 °C. A standard solution of the *S. aureus* was prepared in a density of 10^8 CFU/mL. A 1 mL aliquot of this solution was added into a test tube containing BHI broth medium and the coating samples previously sterilized; each tube with samples was tested independently.

2.8. Antibacterial Activity Determination

After a 24-hour culture, the coatings were gently rinsed with PBS. In order to detach adhering bacteria, the test tubes were vigorously vortexed for 1 min. The solution containing the detached bacteria was diluted in PBS, in a 10-fold proportion, and re-cultivated in agar plates. The agar plate was incubated at 37 °C for 24 h and the number of colony forming units (CFU) was counted using a plate counter. Ten samples of each group were analyzed, and results were compared using one-way analysis of variance (ANOVA) followed by Tukey's multiple comparison test to determine data statistical significance. The bactericidal rate was calculated by the following relation:

$$\text{Bactericidal rate}\,(\%) = \frac{\text{CFUcontrol} \,.\, \text{CFUexperimental}}{\text{CFUcontrol}} .100\% \quad (1)$$

Where CFUcontrol and CFUexperimental are the average of CFU on control sample (CaP) and on experimental samples, respectively.

2.9. Bacterial Morphology

SEM analysis of the adhering bacteria was performed to evaluate the biofilm formation. After 24 h of S. aureus culture in the coatings, a solution of glutaraldehyde 2.5% (Ted Pella) was deposited on the coatings for 4 h to fix the bacteria. After fixation, samples were dehydrated in a series of ethanol solutions for 10 min each and incubated in dexamethyldisilazane (HMDS, Sigma) for 10 min. Prior to observation in SEM, the samples were coated with 20 nm of gold. Bacterial SEM images were recorded with a 45° tilt.

3. RESULTS

3.1. Coating Characterization

The coatings presented a volcano shape porous morphology (Figure **1**), characteristic of coatings obtained by PEO process in calcium and phosphorous containing electrolyte [40,41]. The coatings are 6.2 ± 1.2 µm thick, composed by two layers: a compact inner layer and an external porous layer, region 1 and 2 in Figure **1**, respectively.

Elemental analysis performed by XPS showed the successful incorporation of Ca, P and Ag from the electrolyte, Table **2**. Silver incorporation determined by XPS shows a non-linear relation of Ag concentration on the electrolyte and the ratio Ti/Ag on the coatings (Figure **2**).

The TF-XRD patterns show the formation of two titanium dioxide crystalline phases during the PEO process: Anatase and Rutile (Figure **3**). Additionally, peaks from the titanium substrate can also be observed for all coatings, while peaks from the silver

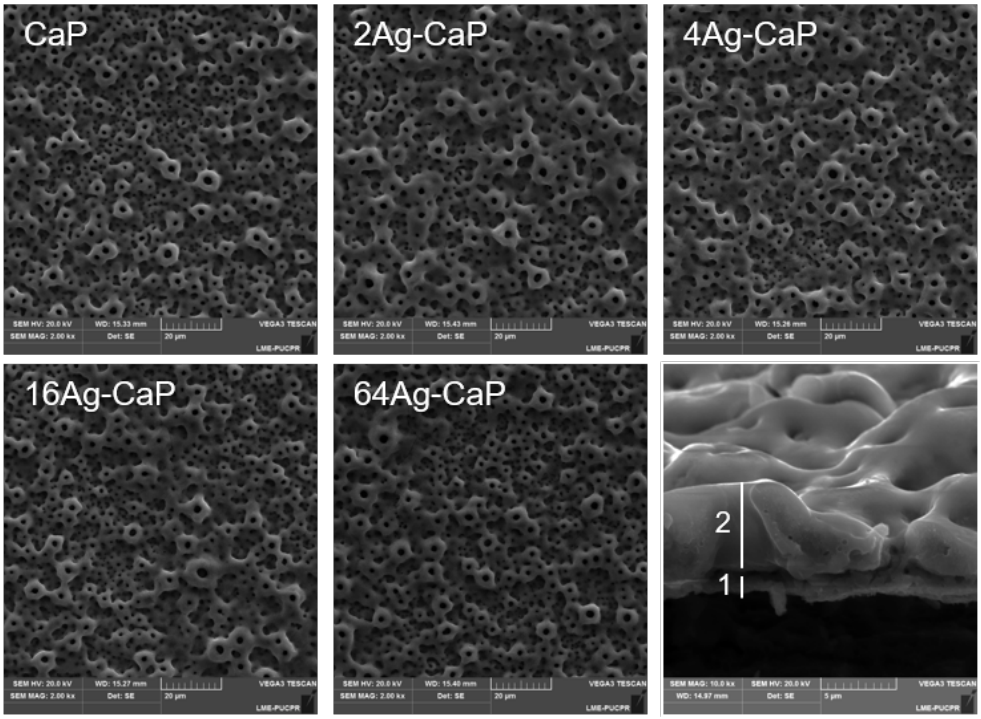

Figure 1: Scanning electron microscopy images from the coatings obtained by PEO. The bottom right image shows the cross-section view from 4Ag-CaP coating.

Table 2: Elemental Composition of the Coatings Assessed by XPS Survey Analysis

Sample name	Elemental composition (at. %)				
	Ti	O	Ca	P	Ag
CaP	6.3	67.4	12.7	13.6	--
2Ag-CaP	7.3	67.7	11	13.8	0.2
4Ag-CaP	4.1	68.7	13.8	12.8	0.6
16Ag-CaP	4.8	65.5	13.8	14.5	1.4
64Ag-CaP	3.7	64.8	13.8	15.2	2.4

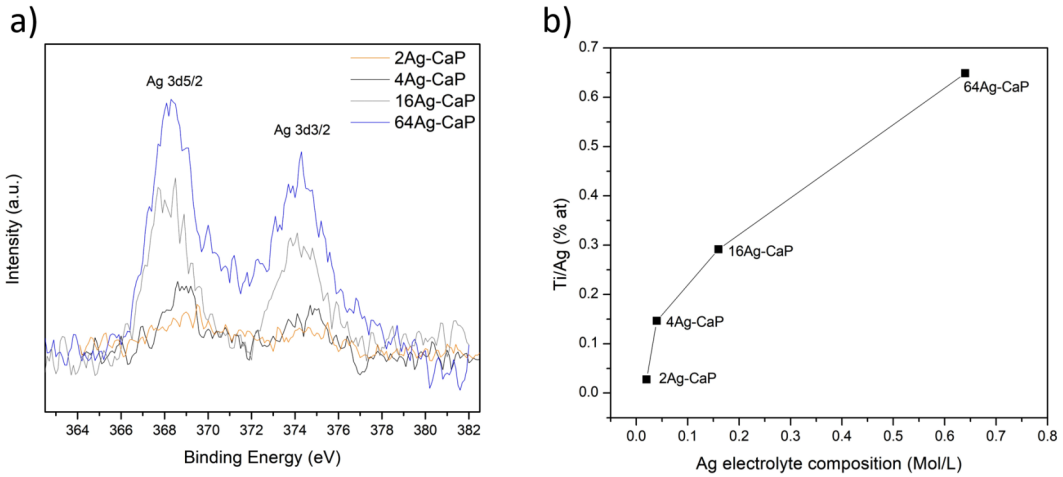

Figure 2: a) High-resolution XPS spectra of Ag 3d and **b**) Ti/Ag ratio incorporated on the coatings by the electrolyte Ag concentration.

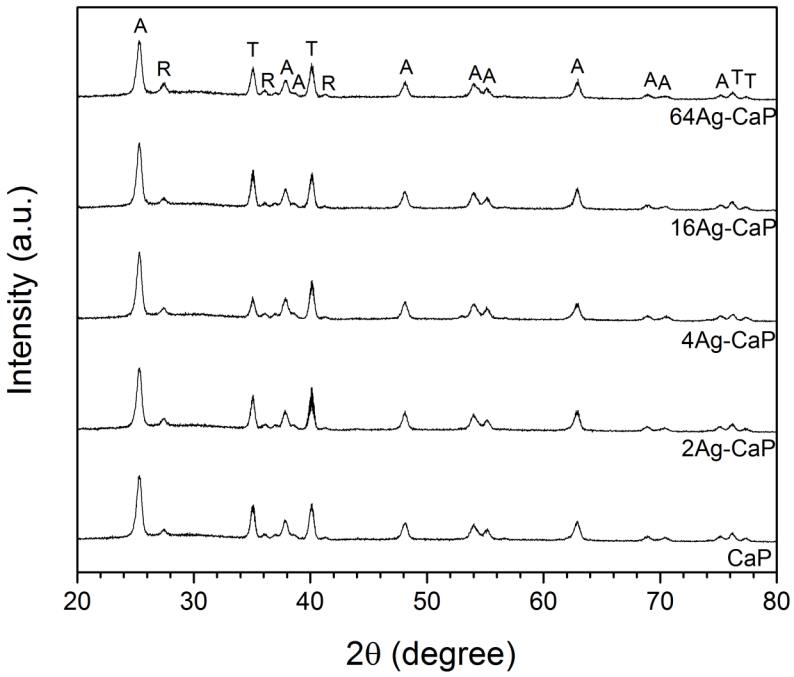

Figure 3: TF-XRD diffraction pattern of the coatings. A, R and T stands for Anatase, Rutile and Titanium, indexed with the ICDD files #01-075-2547, 01-078-4187 and 01-071-4632, respectively.

incorporation were not observed. No difference in the TF- XRD pattern is observed among the coatings, showing the silver incorporation has not affected the crystalline composition.

3.2. Cell Viability, Adhesion and Proliferation

ADSCs viability was not impaired by the silver incorporated coatings, as showed by the percentage of AlamarBlue reduced after 1 and 7 days of culture (Figure **4**). ADSCs are viable on all coatings, with no significant difference among silver containing coatings and the reference group. No cytotoxicity was observed up to 7 days of culture.

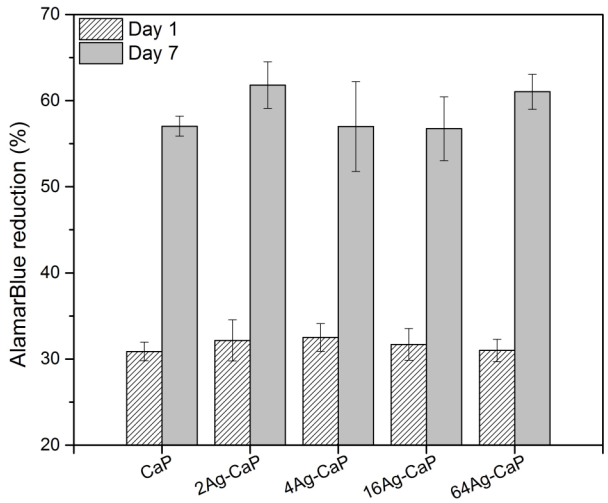

Figure 4: Cell viability on different coatings measured by the reduction percentage of AlamarBlue after 1 and 7 days of ADSCs culture. *p < 0.0001.

After one day of culture, the ADSCs morphology was dependent on the amount of silver in the coatings (Figure **5**). Coatings with higher amounts of silver presented less spread and thinner cells than samples with lower amounts of silver, where a spread star shape ADSCs can be observed (Figure **5**). This difference in cell shape among the groups was not observed after 7 days of culture, since the cells had covered all samples surfaces, indicating the silver presence impacts only the early stage of cell proliferation.

SEM images show ADSC flattened and adhered to the surface coating (Figure **6**). ADSCs presented good affinity with the porous coating, showing cellular extensions toward adjacent cells after just one day of culture. After 7 days of culture, cells have covered the entire coating surface. No difference in cell morphology was observed among the groups, showing that the amount of silver incorporated does not induce deleterious effects in the ADSCs cell adhesion and proliferation.

3.3. Antibacterial Activity

Results of colony forming units counting assay show a significant reduction of S. aureus CFU in groups 4, 16 and 64Ag-CaP after 24 h of incubation,

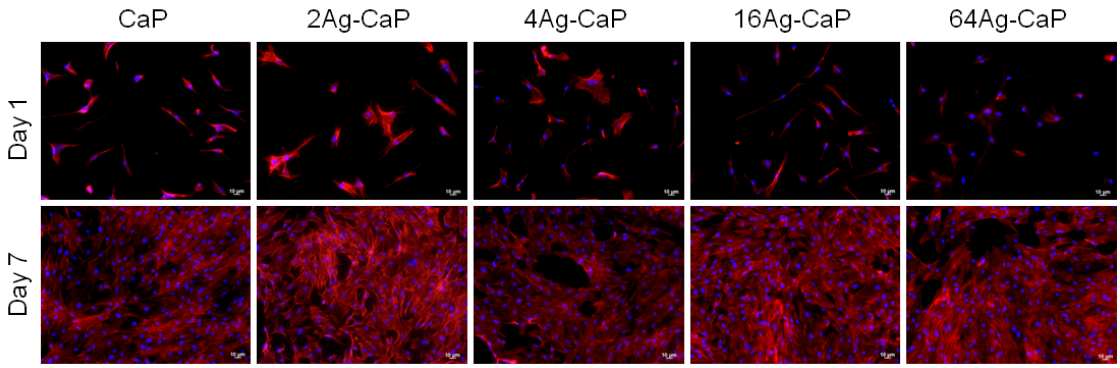

Figure 5: Fluorescence microscope images of ADSCs cultured for 1 and 7 days on different silver containing coatings.

Figure **7**. Surprisingly, the number of CFU has increased on the coating with the smaller amount of silver (group 2Ag-CaP, with 0.2 % Ag), but without significant difference from the reference group. This observation was supported by the bacterial attachment SEM images (Figure **8**). It is possible to observe the biofilm formation on the 2Ag-CaP coating, where the bacteria form a thick layer connected by water channels. On the 4Ag-CaP coating, there are no large bacterial colonies present, just few *S. aureus* are observed.

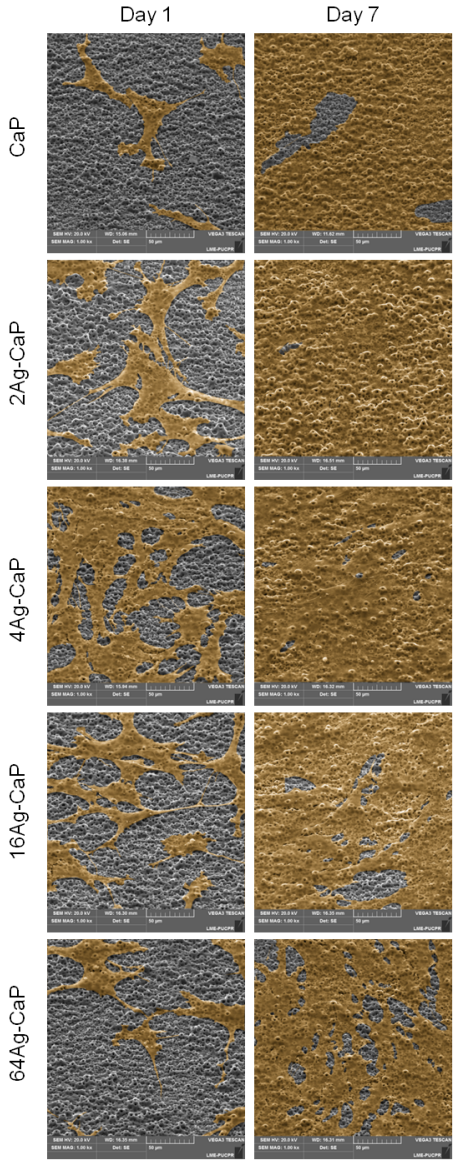

Figure 6: SEM images of ADSCs cultured for 1 and 7 days on different silver containing coatings. For better visualization ADSCs are false-colored orange.

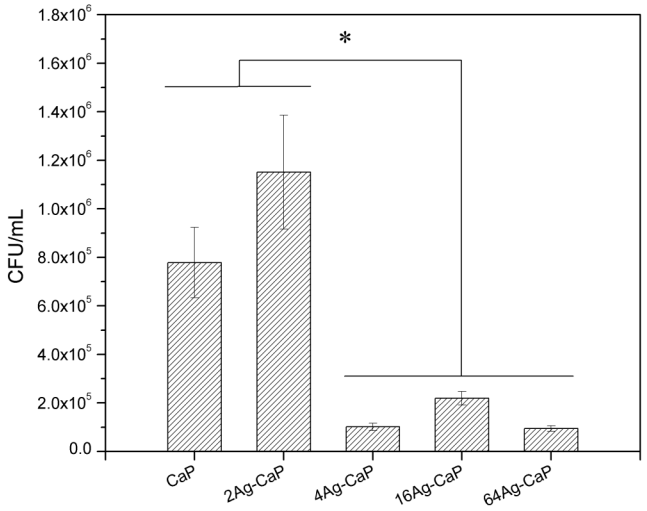

Figure 7: Colony forming units count assessing the antibacterial activity of different coatings against *S. aureus* cultured for 24 h. *p < 0.0001.

Our results show that the 4Ag-CaP coating, containing 0.6% of Ag incorporated, achieves an 87 ± 20% of S. aureus reduction after 24h of culture. Coatings with higher amounts of silver presented similar rates of reduction, 72 ± 15 % and 88 ± 21 % for 16Ag-CaP and 64Ag-CaP, respectively.

4. DISCUSSION

Indwelling implants are susceptible to bacterial contamination not only during the surgery but also

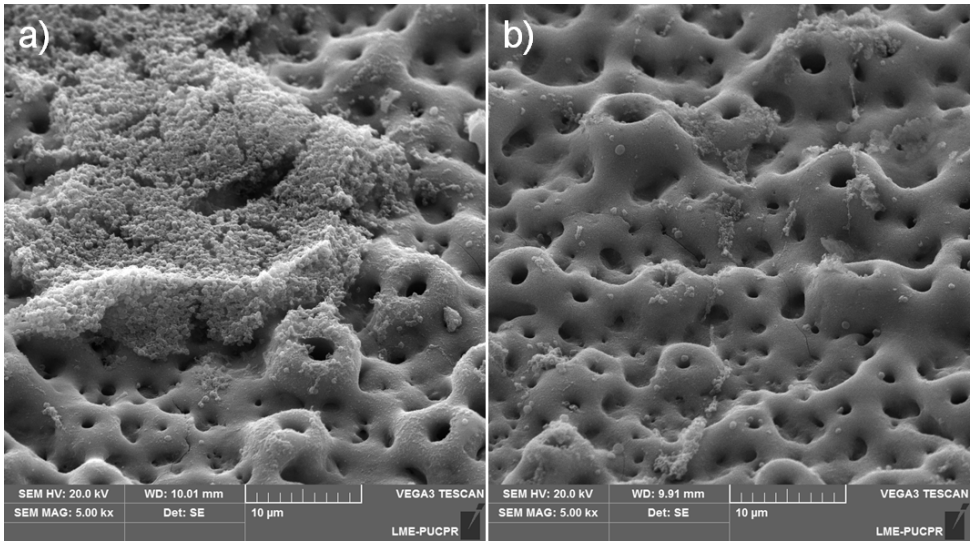

Figure 8: SEM images of *S. aureus* cultured for 24 h on (**a**) 2Ag-CaP and (**b**) 4Ag-CaP coatings.

years after the implantation. Antibacterial coatings based on silver are being proposed as a tool to prevent bacterial infections, although the amount of silver present in the coating must be carefully determined in order not to impair the osseointegration or cause toxic side effects.

In the present study, four silver graded coatings obtained by PEO were evaluated *in vitro* to determine their bactericidal activity and biocompatibility. A hormetic response was observed by increasing of *S. aureus* CFU in the coating containing a small amount of silver. A hormetic dose response occurs when lower doses of toxic agents promote a modest stimulatory response, resulting in an effect that is the opposite of what is expected, as a result of the disruption of the homeostasis [42,43]. Biofilm formation induced by sub-minimal inhibitory concentration of antibiotics or nanoparticles have been extensively reported [43-45]. Although, to the best of our knowledge, this is the first report of hormetic response using bactericidal elements in biomedical coatings, showing the importance of a systematic evaluation of antibacterial agents to be used on implants.

No cytotoxic effects on ADSC were observed when cultured on silver containing coatings, showing that even the higher silver concentration (2.4 % on 64Ag-CaP group) was below the minimum toxic dose. Studies that evaluate the biocompatibility of titania nanotubes doped with silver nanoparticles or silver oxide have also encountered similar results, indicating the possibility to use silver as a valuable antibacterial agent without impairing the eukaryotic cell behavior [46,47]. Cell shape in the early stage of proliferation was dependent on the amount of silver incorporated in the coatings; lower silver amounts lead to a spread star shape ADSCs, while higher silver amounts lead to thinner cells. The cell morphology is closely related to the cell-material affinity. Kilian *et al.* has showed the cell shape influence on cell differentiation, where star shaped stem cells presented an increased signaling related to osteoblast differentiation [48].

Among the tested coatings, the 4Ag-Cap group is selected as the most suitable to be used as a bactericidal coating in implants, since 0.6% Ag in the coating is sufficient to assure the bactericidal activity, and a higher early ADSC spread was observed. Further investigation, evaluating coatings with an incorporated silver concentration between 0.2 % and 0.6 %, i.e. between groups 2Ag-CaP and 4Ag-CaP, is needed to elucidate the minimum bactericidal concentration and to determine the hormetic limit for silver on biomaterial's coatings.

5. CONCLUSIONS

Four different titanium oxide coatings containing silver were obtained by PEO. Unlike other methods to incorporate silver in titanium coatings, PEO is a one-step process that successfully incorporates silver in all coating structure. Silver presence in the coatings has no deleterious effects on ADSC viability and morphology, but cell shape has become less spread on coatings containing more than 1.4% Ag. This study showed that a minimum of 0.6 % of silver incorporated in a titanium oxide coating, along with calcium and phosphorous, is needed to present bactericidal activity against *S. aureus* and no cytotoxicity on ADSCs, being

an attractive bactericidal coating to be used in endosseous implants.

This study showed the importance of evaluating the influence of silver concentration on the biological response of biomedical coatings. A non-expected hormetic response was observed, highlighting the importance of determining a minimum amount of silver needed to assure the bactericidal activity.

ACKNOWLEDGEMENTS

Research reported in this publication was supported by CNPq (Grants #309424/2012-7, #427025/2016-8 and #305715/2016-0).

REFERENCES

[1] Hahn F, Zbinden R, Min K. Late implant infections caused by Propionibacterium acnes in scoliosis surgery. Eur Spine J 2005; 14: 783-788. https://doi.org/10.1007/s00586-004-0854-6

[2] Zimmerli W, Ochsner PE. Management of infection associated with prosthetic joints. Infection 2003; 31: 99-108. https://doi.org/10.1007/s15010-002-3079-9

[3] Renvert S, Roos-Jansaker A-M, Lindahl C, Renvert H, Rutger PG. Infection at titanium implants with or without a clinical diagnosis of inflammation. Clin Oral Implants Res 2007; 18: 509-16. https://doi.org/10.1111/j.1600-0501.2007.01378.x

[4] Darouiche RO. Treatment of infections associated with surgical implants. N Engl J Med 2004; 350: 1422-9. https://doi.org/10.1056/NEJMra035415

[5] Nelson GN, Davis DE, Namdari S. Outcomes in the treatment of periprosthetic joint infection after shoulder arthroplasty: a systematic review. J Shoulder Elbow Surg 2016; 2016; 25(8): 1337-45. https://doi.org/10.1016/j.jse.2015.11.064

[6] Kurtz SM, Lau E, Watson H, Schmier JK, Parvizi J. Economic burden of periprosthetic joint infection in the United States. J Arthroplasty 2012; 27(8 Suppl): 61-5. https://doi.org/10.1016/j.arth.2012.02.022

[7] Willey M, Karam M. Impact of infection on fracture fixation. Orthop Clin North Am 2016; 47(2): 357-64. https://doi.org/10.1016/j.ocl.2015.09.004

[8] Yue C, Zhao B, Ren Y, Kuijer R, van der Mei HC, Busscher HJ, Rochford ETJ. The implant infection paradox: why do some succeed when others fail? Opinion and discussion paper. Eur Cell Mater 2015; 29: 303-13. https://doi.org/10.22203/eCM.v029a23

[9] Berend KR, Lombardi Jr AV, Morris MJ, Bergeson AG, Adams JB, Sneller MA. Two-stage treatment of hip periprosthetic joint infection is associated with a high rate of infection control but high mortality. Clin Orthop Relat Res 2013; 471(2): 510-18. https://doi.org/10.1007/s11999-012-2595-x

[10] Zhao L, Chu PK, Zhang Y, Wu Z. Antibacterial coatings on titanium implants. J Biomed Mater Res Part B Appl Biomater 2009; 91B(1): 470-80. https://doi.org/10.1002/jbm.b.31463

[11] Fielding GA, Roy M, Bandyopadhyay A, Bose S. Antibacterial and biological characteristics of silver containing and strontium doped plasma sprayed hydroxyapatite coatings. Acta Biomater 2012; 8(8): 3144-52. https://doi.org/10.1016/j.actbio.2012.04.004

[12] Fordham WR, Redmond S, Westerland A, Cortes EG, Walker C, Gallagher C, Medina CJ, Waecther F, Lunk C, Ostrum RF, Caputo GA, Hettinger JD, Krchnavek RR. Silver as a bactericidal coating for biomedical implants. Surf Coatings Technol 2014; 253, 52-7. https://doi.org/10.1016/j.surfcoat.2014.05.013

[13] Ewald A, Glückermann SK, Thull R, Gbureck U. Antimicrobial titanium/silver PVD coatings on titanium. Biomed Eng Online 2006; 5: 22. https://doi.org/10.1186/1475-925X-5-22

[14] Ding X, Yang C, Lim TP, Hsu LY, Engler AC, Hedrick JL, Yang YY. Antibacterial and antifouling catheter coatings using surface grafted PEG-b-cationic polycarbonate diblock copolymers. Biomaterials 2012; 33(28): 6593-603. https://doi.org/10.1016/j.biomaterials.2012.06.001

[15] Li H, Gao Y, Li C, Ma G, Shang Y, Sun Y. A comparative study of the antibacterial mechanisms of silver ion and silver nanoparticles by Fourier transform infrared spectroscopy. Vib Spectrosc 2016; 85: 112-21. https://doi.org/10.1016/j.vibspec.2016.04.007

[16] Feng QL, Wu J, Chen GQ, Cui FZ, Kim TN, Kim JO. A mechanistic study of the antibacterial effect of silver ions on Escherichia coli and Staphylococcus aureus. J Biomed Mater Res 2000; 52: 662-68. https://doi.org/10.1002/1097-4636(20001215)52:4<662::AID-JBM10>3.0.CO;2-3

[17] Park HJ, Kim JY, Kim J, Lee JH, Hahn JS, Gu MB, Yoon J. Silver-ion-mediated reactive oxygen species generation affecting bactericidal activity. Water Res 2009; 43(4): 1027-32. https://doi.org/10.1016/j.watres.2008.12.002

[18] Lin B, Luo Y, Teng Z, Zhang B, Zhou B, Wang Q. Development of silver/titanium dioxide/chitosan adipate nanocomposite as an antibacterial coating for fruit storage. LWT Food Sci Technol 2015; 63: 1206-13. https://doi.org/10.1016/j.lwt.2015.04.049

[19] Yoon KY, Byeon JH, Park CW, Hwang J. Antimicrobial effect of silver particles on bacterial contamination of activated carbon fibers. Environ Sci Technol 2008; 42(4): 1251-55. https://doi.org/10.1021/es0720199

[20] Miaśkiewicz-Peska E, Łebkowska M. Effect of antimicrobial air filter treatment on bacterial survival. Fibres Text East Eur 2011; 84: 73-7.

[21] Lv Y, Liu H, Wang Z, Liu S, Hao L, Sang Y, Liu D, Wang J, Boughton RI. Silver nanoparticle-decorated porous ceramic composite for water treatment. J Memb Sci 2009; 331: 50-6. https://doi.org/10.1016/j.memsci.2009.01.007

[22] de Moura MR, Mattoso LHC, Zucolotto V. Development of cellulose-based bactericidal nanocomposites containing silver nanoparticles and their use as active food packaging. J Food Eng 2012; 109(3) 520-24. https://doi.org/10.1016/j.jfoodeng.2011.10.030

[23] Paladini F, Cooper IR, Pollini M. Development of antibacterial and antifungal silver-coated polyurethane foams as air filtration units for the prevention of respiratory diseases. J Appl Microbiol 2014; 116(3): 710-17. https://doi.org/10.1111/jam.12402

[24] Piao MJ, Kang KA, Lee IK, Kim HS, Kim S, Choi JY, Choi J, Hyun JW. Silver nanoparticles induce oxidative cell damage in human liver cells through inhibition of reduced glutathione and induction of mitochondria-involved apoptosis. Toxicol Lett 2011; 201(1): 92-100. https://doi.org/10.1016/j.toxlet.2010.12.010

[25] Xue Y, Zhang T, Zhang B, Gong F, Huang Y, Tang M. Cytotoxicity and apoptosis induced by silver nanoparticles in human liver HepG2 cells in different dispersion media. J Appl Toxicol 2016; 36(3): 352-60. https://doi.org/10.1002/jat.3199

[26] Trop M, Novak M, Rodl S, Hellbom B, Kroell W, Goessler W. Silver-coated dressing acticoat caused raised liver enzymes and argyria-like symptoms in burn patient. J Trauma Inj Infect Crit Care 2006; 60(3): 648-52. https://doi.org/10.1097/01.ta.0000208126.22089.b6

[27] Jiravova J, Tomankova KB, Harvanova M, Malina L, Malohlava J, Luhova L, Panacek A, Manisova B, Kolarova H. The effect of silver nanoparticles and silver ions on mammalian and plant cells *in vitro*. Food Chem Toxicol 2016; 96: 50-61. https://doi.org/10.1016/j.fct.2016.07.015

[28] Sakai N, Aoki M, Miyazawa S, Akita M, Takezaki S, Kawana S. A case of generalized argyria caused by the use of silver protein as a disinfection medicine. Acta Derm Venereol 2007; 87(2): 186-7. https://doi.org/10.2340/00015555-0180

[29] Karakasli A, Hapa O, Akdeniz O, Havitcioğlu H. Dermal argyria: Cutaneous manifestation of a megaprosthesis for distal femoral osteosarcoma. Indian J Orthop 2014; 48(3): 326-8. https://doi.org/10.4103/0019-5413.132528

[30] Raphel J, Holodniy M, Goodman SB, Heilshorn SC. Multifunctional coatings to simultaneously promote osseointegration and prevent infection of orthopaedic implants. Biomaterials 2016; 84: 301-14. https://doi.org/10.1016/j.biomaterials.2016.01.016

[31] AshaRani PV, Low Kah Mun G, Hande MP, Valiyaveettil S. Cytotoxicity and genotoxicity of silver nanoparticles in human cells. ACS Nano 2009; 3(2): 279-90. https://doi.org/10.1021/nn800596w

[32] Yerokhin AL, Nie X, Leyland A, Matthews A, Dowey SJ. Plasma electrolysis for surface engineering. Surf Coatings Technol 1999; 122(2-3): 73-93. https://doi.org/10.1016/S0257-8972(99)00441-7

[33] Zhang W, Du K, Yan C, Wang F. Preparation and characterization of a novel Si-incorporated ceramic film on pure titanium by plasma electrolytic oxidation. Appl Surf Sci 2008; 254(16): 5216-23. https://doi.org/10.1016/j.apsusc.2008.02.047

[34] Krupa D, Baszkiewicz J, Zdunek J, Smolik J, Słomka Z, Sobczak JW. Characterization of the surface layers formed on titanium by plasma electrolytic oxidation. Surf Coatings Technol 2010; 205(6): 1743-49. https://doi.org/10.1016/j.surfcoat.2010.05.015

[35] Laurindo CAH, Torres RD, Mali SA, Gilbert JL, Soares P. Incorporation of Ca and P on anodized titanium surface: Effect of high current density. Mater Sci Eng C 2014; 37(1): 223-31. https://doi.org/10.1016/j.msec.2014.01.006

[36] Quintero D, Galvis O, Calderón JA, Castaño JG, Echeverría F. Effect of electrochemical parameters on the formation of anodic films on commercially pure titanium by plasma electrolytic oxidation. Surf Coatings Technol 2014; 258: 1223-31. https://doi.org/10.1016/j.surfcoat.2014.06.058

[37] Ribeiro AR, Oliveira F, Boldrini LC, Leite PE, Falagan-Lotsch P, Linhares ABR, Zambuzzi WF, Fragneaud B, Campos APC, Gouvêa CP, Archanjo BS, Achete CA, Marcantonio E, Rocha LA, Granjeiro JM. Micro-arc oxidation as a tool to develop multifunctional calcium-rich surfaces for dental implant applications. Mater Sci Eng C Mater Biol Appl 2015; 54:196-206. https://doi.org/10.1016/j.msec.2015.05.012

[38] Sul Y-T, Johansson CB, Albrektsson T. Oxidized titanium screws coated with calcium ions and their performance in rabbit bone. Int J Oral Maxillofac Implants 2002; 17: 625-34.

[39] Song WH, Jun YK, Han Y, Hong SH. Biomimetic apatite coatings on micro-arc oxidized titania. Biomaterials 2004; 25: 3341-49. https://doi.org/10.1016/j.biomaterials.2003.09.103

[40] Li Y, Lee IS, Cui FZ, Choi SH. The biocompatibility of nanostructured calcium phosphate coated on micro-arc oxidized titanium. Biomaterials 2008; 29(13): 2025-32. https://doi.org/10.1016/j.biomaterials.2008.01.009

[41] Ishizawa H, Ogino M. Formation and characterization of anodic titanium oxide films containing Ca and P. J Biomed Mater Res 1995; 29(1): 65-72. https://doi.org/10.1002/jbm.820290110

[42] Calabrese EJ. Hormesis: a revolution in toxicology, risk assessment and medicine. EMBO Rep 2004; 5(S1): S37-S40. https://doi.org/10.1038/sj.embor.7400222

[43] Iavicoli I, Fontana L, Leso V, Calabrese EJ. Hormetic dose-responses in nanotechnology studies. Sci Total Environ 2014; 487: 361-74. https://doi.org/10.1016/j.scitotenv.2014.04.023

[44] Kaplan JB. Antibiotic-induced biofilm formation. Int J Artif Organs 2011; 34(9): 737-51. https://doi.org/10.5301/ijao.5000027

[45] Davies J, Spiegelman GB, Yim G. The world of subinhibitory antibiotic concentrations. Curr Opin Microbiol 2006; 9(5): 445-53. https://doi.org/10.1016/j.mib.2006.08.006

[46] Gao A, Hang R, Huang X, Zhao L, Zhang X, Wang L, Tang B, Ma S, Chu PK. The effects of titania nanotubes with embedded silver oxide nanoparticles on bacteria and osteoblasts. Biomaterials 2014; 35(13): 4223-35. https://doi.org/10.1016/j.biomaterials.2014.01.058

[47] Lan MY, Liu CP, Huang HH, Lee SW. Both enhanced biocompatibility and antibacterial activity in Ag-decorated TiO2 nanotubes. PLoS One 2013; 8(10): e75364. https://doi.org/10.1371/journal.pone.0075364

[48] Kilian KA, Bugarija B, Lahn BT, Mrksich M. Geometric cues for directing the differentiation of mesenchymal stem cells. PNAS 2010; 107(11): 4872-77. https://doi.org/10.1073/pnas.0903269107

Received on 07-02-2018 Accepted on 30-03-2018 Published on 11-04-2018

DOI: http://dx.doi.org/10.12970/2311-1755.2018.06.02